Supplementary section

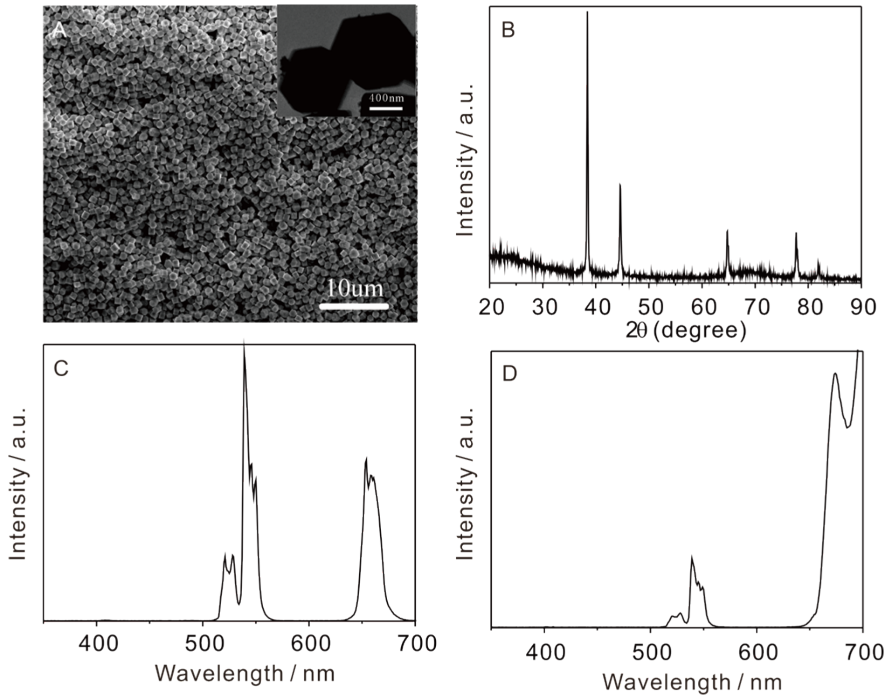

Fig. S1 (A) SEM image of $NaYF_4$:Yb,Er NCs (inset: the corresponding TEM image). (B) XRD patterns of $NaYF_4$:Yb,Er NCs. UC emission spectrum of $NaYF_4$:Yb,Er NCs under (C) 980 nm and (D) 808 nm excitation, respectively.

The uniform $NaYF_4$:Yb,Er NCs were synthesized by a simple hydrothermal method using trisodium citrate as a capping agent.[1, 2] As shown in Fig. S1A, the $NaYF_4$:Yb,Er NCs are very uniform, and with an average side length of ~600 nm was clearly revealed by the TEM image (the inset of Fig. S1A). The XRD patterns of $NaYF_4$:Yb,Er NCs are shown in Fig. S1B. Most of the XRD diffraction peaks of the samples are in good agreement with the standard values for the hexagonal-phase $NaFY_4$ crystals (JCPDS files No.16-0334).

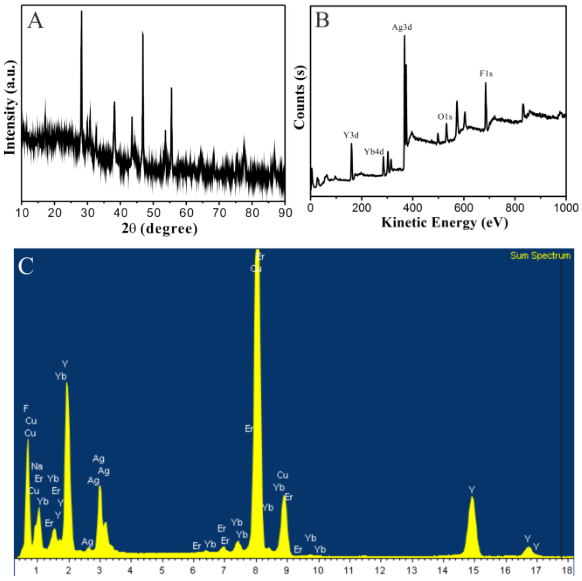

Fig. S2 (A) XRD patterns of UC@Ag NCs. (B)XPS spectrum of the $NaYF_4$:Yb,Er @Ag nanocrystals. (C) EDAX spectrum of the UC@Ag NCs.

Fig. S2A shows the XRD patterns of $NaYF_4$:Yb,Er@Ag, the new peaks at 2θ= 38.0, 44.2, 64.4, and 77.3° are consistent with the face Ag (JCPDS 87-0720). The composite materials were also characterized by XPS shown in the Fig. S2B, the strong Ag 3d peak at 372 eV can prove the presence of Ag.

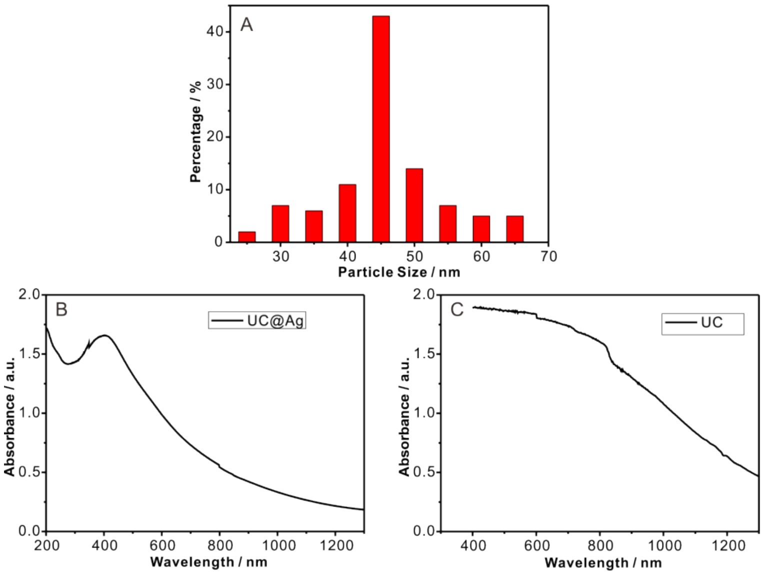

Fig. S3 (A) Particle size distribution histograms of Ag loaded on UC@Ag. (B) UV-vis diffused reflectance absorption spectra of UC@Ag substrate. (C) UV-vis diffused reflectance absorption spectra of $NaYF_4$,

The UV-vis diffused reflectance absorption spectra of dry UC and UC@Ag substrate also shown in Fig. S3B and C. Deducting the absorption of UC, we find that the LSPR of Ag NPs decorated on $NaYF_4$:Yb,Er didn't observed red shift phenomenon. It may because the size of Ag NPs decorated on $NaYF_4$:Yb,Er is much smaller than that of UC, the interparticle gaps are larger than that of the ML-Ag and the density is lower than that of the ML-Ag, which will reduce the coupling of the Ag NPs. So the deposition of Ag nanoparticles on the $NaYF_4$ can't lead to the red shift of LSPR and the 785 nm laser can't directly excite the LSPR of Ag NPs.

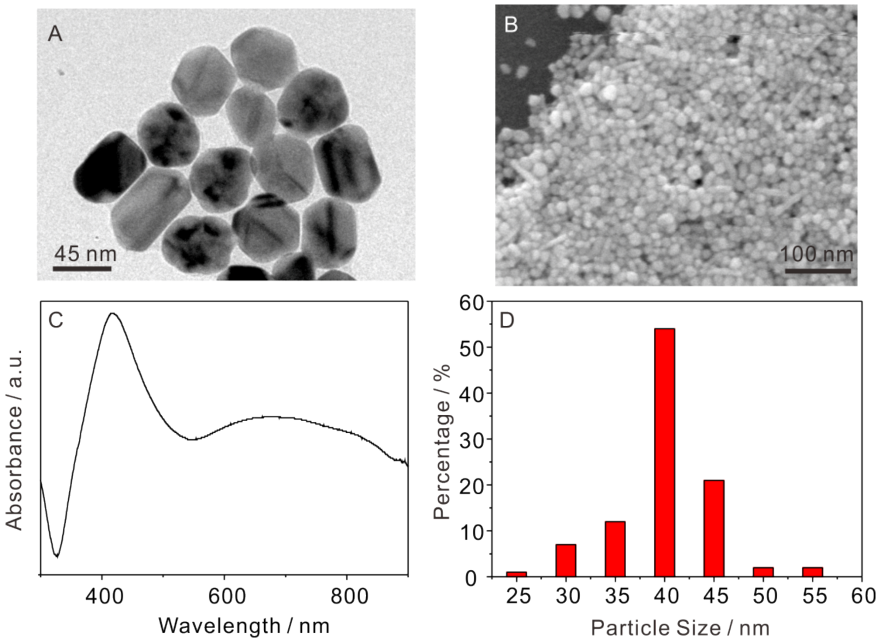

Fig. S4 TEM (A) and SEM (B) image of Ag NPs. (C) UV-vis diffused reflectance absorption spectra of Ag substrate. (D) Particle size distribution histograms of Ag NPs.

As a control, the Ag nanoparticle sols were prepared according to the classical citrate reduction method. The LSPR peak of Ag sols located at 415 nm (Fig. S4C) and the statistical average diameter of Ag NPs are about 40±11 nm (Fig. S4A and D). 5 μL of the 100-fold concentrated Ag sols dried in air on the surface of silicon wafer can form the multilayers of Ag NPs, which were used as the reference substrate. The UV-vis diffused reflectance absorption spectra of dry ML- Ag substrate showing the broad absorption covered the visible light range (Fig. S4C). The red shift of the LSPR of ML-Ag may due to the formation of very big clusters and decrease the interparticle gaps when the substrate is dried.

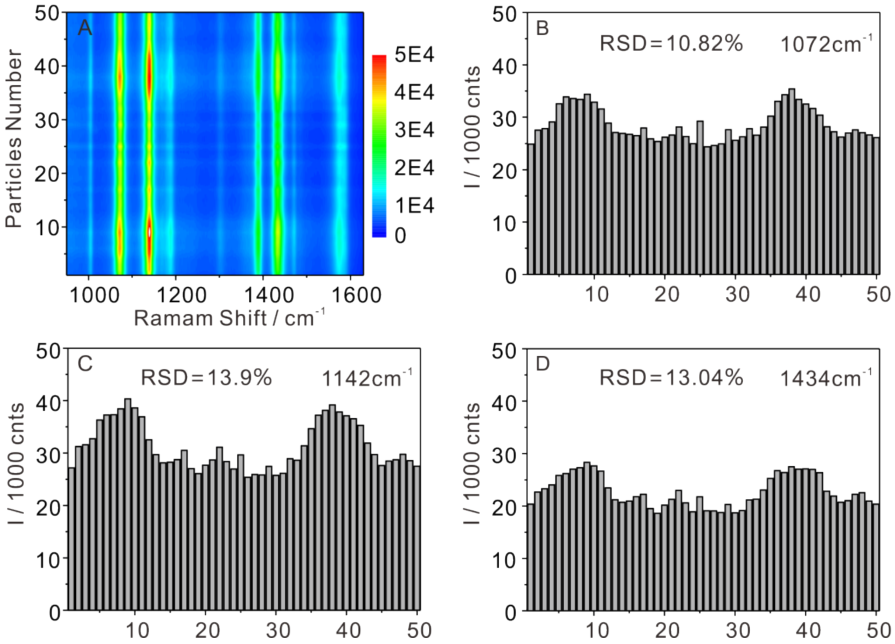

Fig. S5 A series of SERS spectra of 10^{-6} M pATP molecules collected on 50 randomly selected particles of the UC@Ag and the intensities of the main vibrations of pATP.

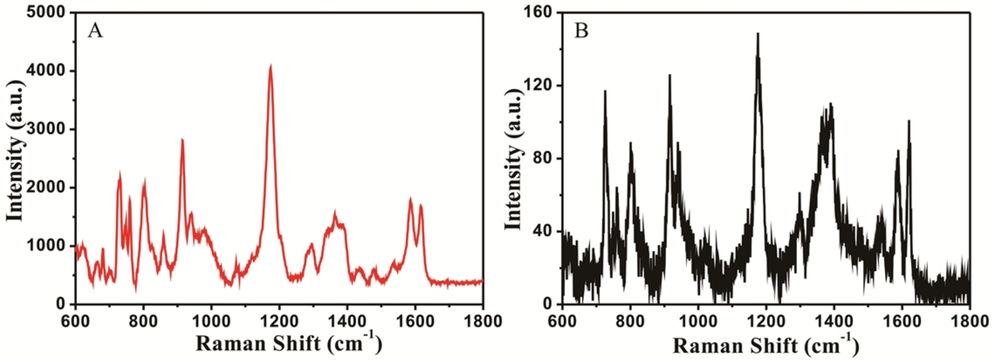

Fig. S6 The SERS spectra of 10^{-5}M CV by the enhancement of (A) UC @Ag and (B) Ag on a silicon substrate.

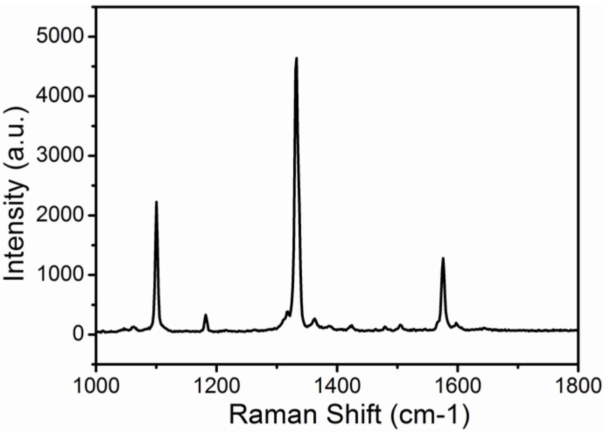

Fig. S7 The normal Raman spectrum of pNTP powder.

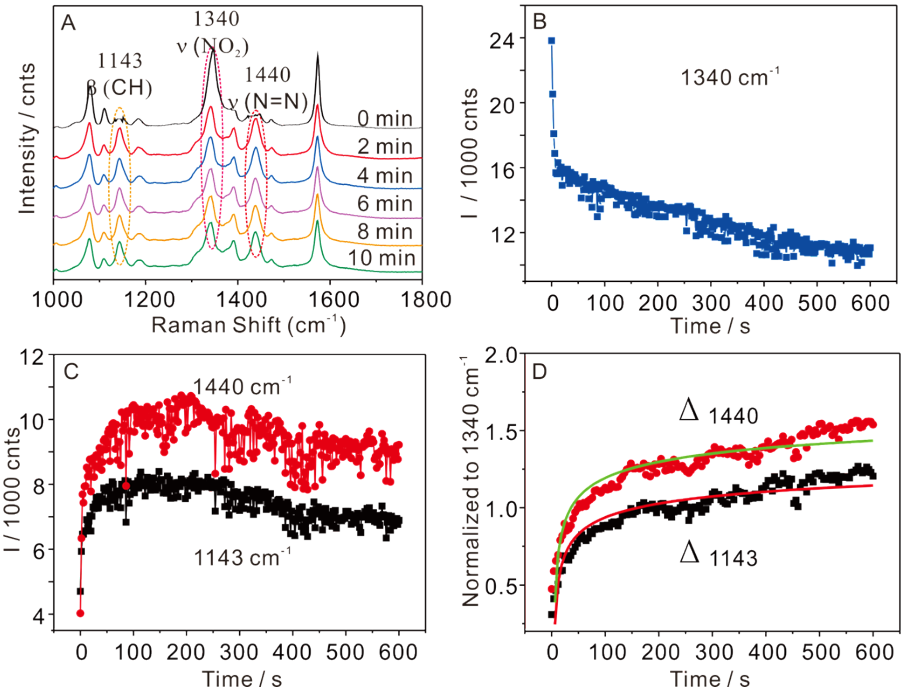

Fig.S8 Time-dependent SERS spectra of pNTP under continuous exposure of a 532 nm laser. The spectra were collected for UC@ Ag particles, with an integration time of 2 s. The intensity of (B) 1340 cm^{-1}, (C) 1440 cm^{-1} and 1143 cm^{-1} with different illumination time. (D) The illumination time-dependent relative intensity of 1440 cm^{-1} and 1143 cm^{-1} to 1340 cm^{-1}.

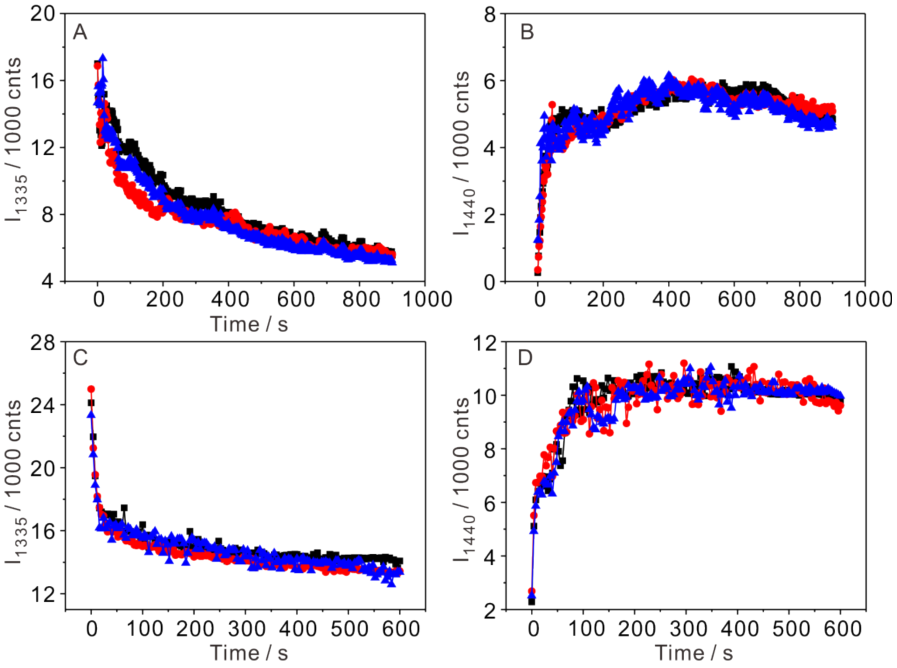

Fig. S9 A series of time-dependent SERS spectra of pNTP collected on 3 randomly selected particles. The intensity of 1335 cm^{-1} and 1440 cm^{-1} with different illumination time under continuous exposure of a 785 nm laser (A), (B) and 532 nm laser (C), (D).

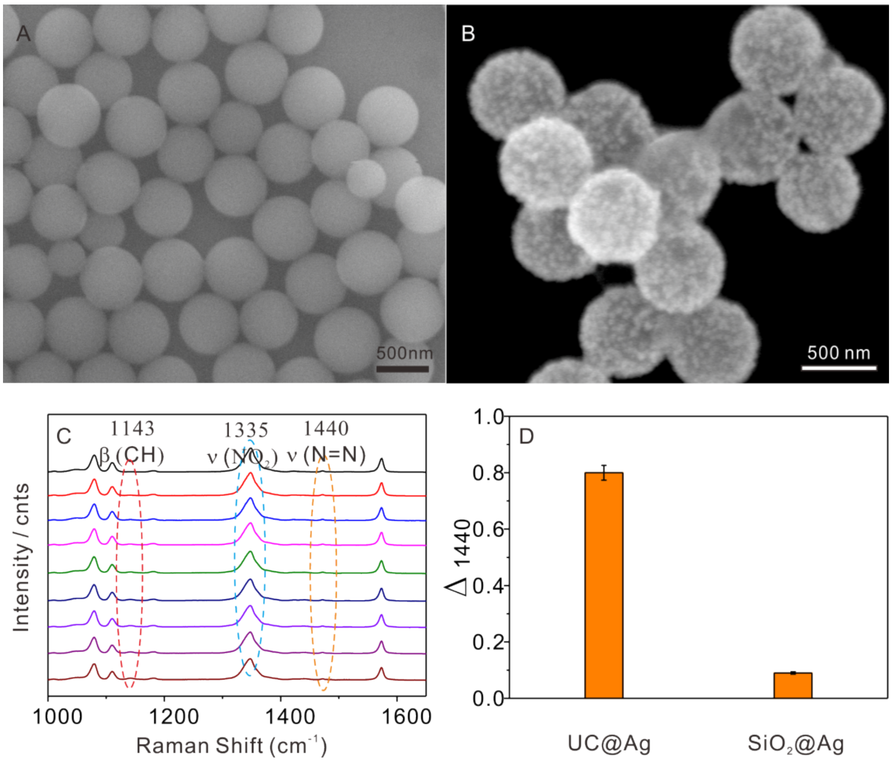

Fig S10 (A) SEM image of SiO$_{2,}$ (B) SEM image of SiO$_2$@Ag. (C) Time-dependent SERS spectra of pNTP under continuous exposure to a 785 nm laser. The spectra were collected on UC@ Ag particles, with an integration time of 2 s. (D) The Δ_{1440} curves under continuous exposure to the lasers of 785 nm on UC@Ag and SiO$_2$@Ag, respectively.

As shown in Fig. S10A-B, the SiO$_2$ are very uniform, and with an average side length of ~600 nm, the Ag NPs had been successfully decorated on SiO$_{2,}$ labeled as SiO$_2$@Ag. A time-course SERS mapping was performed on a single-particle of SiO$_2$@Ag under continuous exposure to a 785 nm laser (Fig. S10C). As the exposure time increased, the SERS intensity of ν(NO$_2$) stretching mode at 1335 cm^{-1}, the ν(N=N) stretching mode at 1385 and the β(CH) stretching mode 1440 cm^{-1} had little changed. The Δ_{1440} reached a relatively stable value of only 0.085 after about 300 s illumination, and the UC@Ag made a value of about 0.75 (Fig. 6B). It can be estimated that the Δ_{1440} of UC@Ag nm is about 8.8 times that of SiO$_2$@Ag under the 785 nm excitation. This difference is attributed to the function of the UC.

References:

1. S. Schietinger, T. Aichele, H. Q. Wang, T. Nann and O. Benson, *Nano Lett*, 2010, **10**, 134-138.
2. Y. J. Sun, Y. Chen, L. J. Tian, Y. Yu, X. G. Kong, J. W. Zhao and H. Zhang, *Nanotechnology*, 2007, **18**.